Submillennial variations in ocean conditions during deglaciation based on diatom assemblages from the southwest Atlantic

Claire S. Allen,[1] Jennifer Pike,[2] Carol J. Pudsey,[1] and Amy Leventer[3]

[1]   We present a high-resolution paleoceanographic record of deglaciation based on diatom assemblages from a core located just south of the Polar Front in the southwest Atlantic. Core KC073 is from a sediment drift at the mouth of the Falkland Trough and contains sediments from the Last Glacial Maximum (LGM) to present, dated using radiocarbon dates on bulk organic matter and radiolarian stratigraphy. The site lies along the path of the Antarctic Circumpolar Current (ACC) and immediately downstream of where North Atlantic Deep Water (NADW) is entrained into the ACC. Significant variations in ocean conditions are reflected in high-amplitude changes in diatom concentrations and assemblage composition. The diatom assemblage at the LGM indicates that winter sea ice extent was at least 5° farther north than present until at least 19.0 ka (calendar years) and summer sea ice may have occasionally extended over the site, but for the most part it lay to the south. During deglaciation, *Chaetoceros* resting spores (CRS) dominate the diatom assemblage with valve concentrations in excess of 500×10^6 valves per gram. Submillennial-scale variations in the numbers of CRS and *Thalassiosira antarctica* occur throughout the late deglacial and dominate the changes in diatom concentration. We propose that the influx of CRS is controlled by the flow of NADW over the Falkland Plateau. As such our data provide unique evidence that NADW impacted on this sector of the Southern Ocean during deglaciation. During the Holocene the sedimentation rate dramatically reduced. We suggest that the ACC flow increased over the site and inhibited settling and winnowed the surface sediments.

1.   Introduction

[2]   Detailed reconstructions of late Quaternary ocean and climate variability in the Northern Hemisphere greatly outnumber those of the Southern Hemisphere. High-resolution marine records from the North Atlantic have been correlated with ice core and terrestrial records across the Northern Hemisphere and provide the basis for a detailed picture of climate variability during the late Quaternary [*Waelbroeck et al.*, 2001]. In contrast, Southern Hemisphere reconstructions suffer from a shortage of high-resolution records and, for those that exist, a poorly constrained chronology. Recent work in the Antarctic Peninsula and Prydz Bay has addressed this paucity of records but most studies are limited to the Holocene period [*Leventer et al.*, 1996; *Domack et al.*, 1998; *Taylor et al.*, 2001; *Leventer et al.*, 2002; *Sjunneskog and Taylor*, 2002; *Warner and Domack*, 2002]. The importance of developing our understanding of southern high-latitude records is becoming greater as more complex interactions between the global ocean and the atmosphere are increasingly apparent from reconstructions and modeling. The thermohaline

"conveyor" of the ocean is a highly dynamic and effective climate regulator [*Bond*, 1995; *Broecker*, 1997; *Wang et al.*, 2002] and the Southern Ocean plays an important role in the propulsion and propagation of this circulation [*Macdonald*, 1998; *Hellmer and Beckmann*, 2001; *Seidov et al.*, 2001]. Reconstructing the fluctuations of the late Quaternary climate of the Southern Ocean will help to define the role the Southern Ocean plays in the global climate system.

[3]   Surveys of the Scotia Sea have revealed a complex oceanography and dynamic current flows [*Arhan et al.*, 2002; *Garabato et al.*, 2002]. Water masses entrained in the Antarctic Circumpolar Current (ACC) follow a complex path across the Scotia Sea region, through the North Scotia Ridge and emerge into the South Atlantic strongly modified by the mixing induced by local bathymetry. Core KC073, discussed here, was taken from a sediment drift at the mouth of the Falkland Trough, northwest of South Georgia (Figure 1), south of the Polar Front and approximately 600 km north of the average winter sea ice extent. The site lies along the path of the ACC, close to the Polar Front (PF) and immediately down stream of where North Atlantic Deep Water (NADW) is entrained into the ACC (Figure 2). The core site is ideally placed to record signals of variations in the flow regimes of the ACC and NADW within the Southern Ocean. These water masses play crucial roles in the global ocean circulation and results discussed here will provide important new data on their responses to climate changes of the late Quaternary.

---

[1]British Antarctic Survey, Cambridge, UK.
[2]Department of Earth Sciences, Cardiff University, Cardiff, UK.
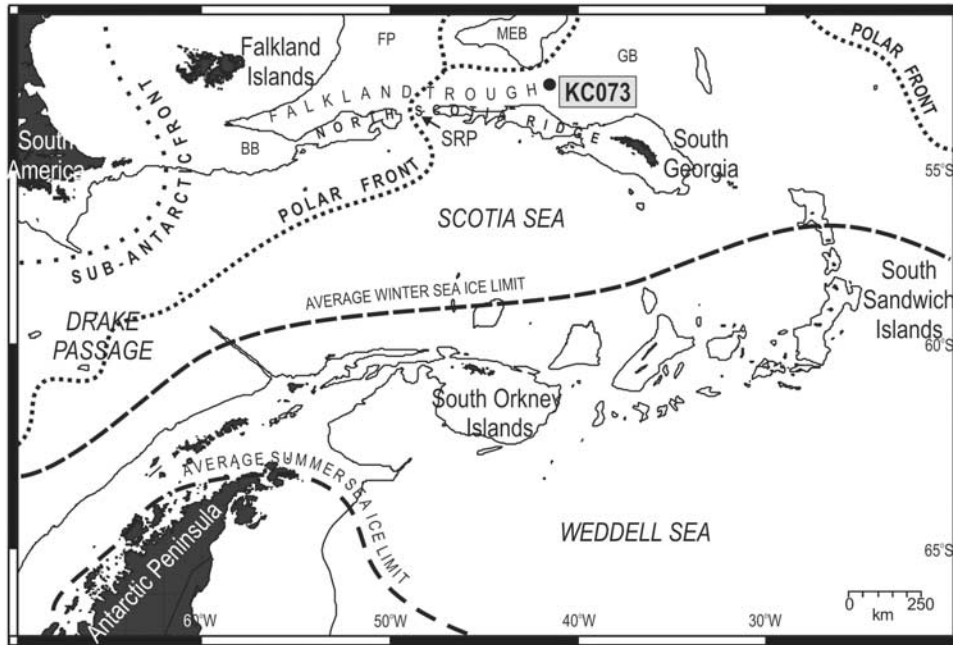[3]Department of Geology, Colgate University, Hamilton, New York, USA.

Figure 1. Map showing core location and bathymetric features mentioned in the text. The 2000 m depth contour is marked. Abbreviations are BB, Burdwood Bank; FP, Falkland Plateau; MEB, Maurice Ewing Bank; GB, Georgia Basin; and SRP, Shag Rocks Passage. The Polar Front and Sub-Antarctic Front are marked with dotted lines, and the average summer and winter sea ice extent are marked with dashed lines. Map is based on data from the *Australian Antarctic Data Centre* [2000] and *Arhan et al.* [2002].
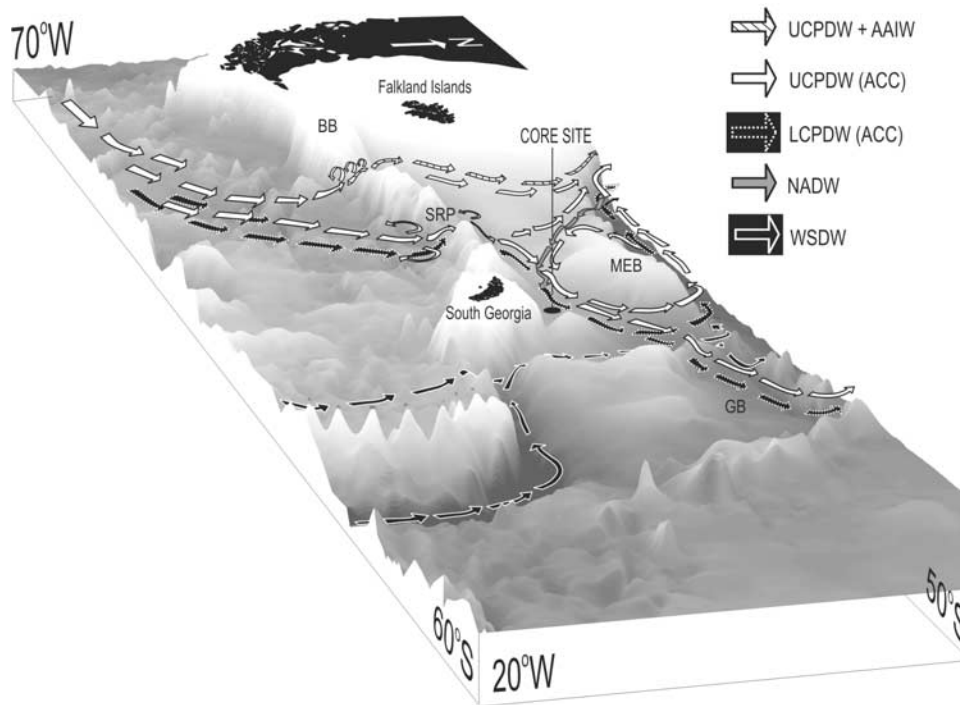

Figure 2. Schematic of the regional water masses and main current pathways of the Falkland Trough based on data from the ALBATROSS project [*Arhan et al.*, 2002]. The black ellipse indicates the core site of KC073. Abbreviations are UCPDW/LCPDW, Upper/Lower Circumpolar Deep Water; NADW, North Atlantic Deep Water; WSDW, Weddell Sea Deep Water; AAIW, Antarctic Intermediate Water; BB, Burdwood Bank; MEB, Maurice Ewing Bank; GB, Georgia Basin; and SRP, Shag Rocks Passage. See color version of this figure in the HTML.

[4] Marine diatom assemblages are widely used as a proxy tool in paleoceanographic reconstructions. Diatoms are particularly effective proxies at high southern latitudes where other common marine microfossils are scarce (e.g., foraminifera) as they are well preserved, abundant and diverse throughout the Southern Ocean and respond to small changes in oceanographic conditions [*Pichon et al.*, 1987; *Leventer and Dunbar*, 1996; *Zielinski and Gersonde*, 1997; *Crosta et al.*, 1998a; *Cunningham and Leventer*, 1998; *Zielinski et al.*, 1998; *Gersonde and Zielinski*, 2000; *Crosta et al.*, 2004].

2. Oceanographic Setting

[5] The Falkland Trough extends eastward to the north of the North Scotia Ridge, from north of the Burdwood Bank to the Georgia Basin in the South Atlantic (Figure 1). It is over 3500 m deep along its axis and is bounded to the north by the Falkland Plateau and the Maurice Ewing Bank. The North Scotia Ridge forms the southern boundary of the trough. The routes of the main water masses in this region are shown in Figure 2 (based on *Arhan et al.* [2002]).

[6] Circulation in the Scotia Sea is dominated by the eastward flowing ACC [*Orsi et al.*, 1995]. Circumpolar Deep Water (CPDW) is the main body of water associated with the ACC and is usually divided into an upper and lower component (UCPDW and LCPDW respectively). The ACC is the largest current system in the world and transfers water between the major basins of the Pacific, Indian and Atlantic Oceans. The main flow runs broadly parallel to the Polar Front and extends to depths of 3000–3500 m. In the Scotia Sea region, bathymetry controls and modifies the path of the currents, not only confining the route of deep water, but also producing meanders and eddies which enhance mixing and result in pockets of water crossing the Polar Front [*Peterson and Whitworth*, 1989; *Arhan et al.*, 2002]. Shag Rocks Passage at 48°W in the North Scotia Ridge is the main deepwater route into the Falkland Trough, and constrains the flow of Antarctic deep waters into the South Atlantic. Another important break in the ridge lies east of Burdwood Bank and permits the northward flow of Antarctic Intermediate Water (AAIW) and UCPDW across the western Falkland Plateau into the Argentine Basin (Figure 2). Other gaps in the ridge system allow surface water flow but are too shallow to permit the passage of deepwater masses.

[7] The Falkland Plateau deflects most of the UCPDW and LCPDW that flows northward through Shag Rocks Passage into the Falkland Trough and eastward toward the Georgia Basin. A second branch of UCPDW overflows the Falkland Plateau sill west of the Maurice Ewing Bank and flows directly into the Argentine Basin where it becomes incorporated into the western boundary current. Of the waters reaching the Georgia Basin, most flow eastward through it; however, some LCPDW flows north and westward into the Argentine Basin. A core of UCPDW circulates the rim of the Maurice Ewing Bank and entrains southerly flowing NADW along the Falkland Escarpment and over the Falkland Plateau into the Falkland Trough (Figure 2) [*Arhan et al.*, 2002].

[8] The frontal systems in this region are characterized by divergent paths following the constricted flow through the Drake Passage. The Sub-Antarctic Front (SAF), after crossing the North Scotia Ridge, hugs the continental shelf before merging with the boundary current of the Argentine Basin [*Peterson and Whitworth*, 1989; *Orsi et al.*, 1995; *Arhan et al.*, 2002; *Garabato et al.*, 2002]. *Arhan et al.* [2002] have clarified the dynamics of the Polar Front (PF) in the region of the Falkland Plateau. Although previous studies observed the PF to the south or west of the Maurice Ewing Bank, *Arhan et al.* [2002] demonstrate that rather than an episodic migration of a single front between these two routes there is a bifurcation in the PF north of Shag Rocks Passage. They suggest that the relative strengths of these branches (one over the sill of the Falkland Plateau and one along the axis of the Falkland Trough) may vary through time, and meandering between them may result in extensions of the PF crossing the Maurice Ewing Bank.

[9] The high-resolution diatom record presented here is used to reconstruct the ocean and climate dynamics of the Falkland Trough and northern Scotia Sea, since the Last Glacial Maximum (LGM).

3. Materials and Methods

[10] The core (KC073) is a 2.8 m long kasten core, collected from a depth of 3760 m in 1995 during cruise JR04 of the RRS *James Clark Ross* (52°09.2′S, 41°10.7′W). The sediments consist of muddy diatom ooze and diatom-bearing silt in the lower part of the core (2.88–2.14 m) grading up to almost pure diatom ooze in the upper part (2.14–0.0 m).

[11] The chronology for core KC073 is based on the radiolarian stratigraphic marker, *Cycladophora davisiana* and nine radiocarbon dates (Figure 3). *Hays et al.* [1976] showed that the first down-core peak of *C. davisiana* is synchronous around the Antarctic and sub-Antarctic and has been broadly correlated with the LGM [*Hays et al.*, 1976; *Brathauer et al.*, 2001]. In KC073 the largest peak in *C. davisiana* (>22%) occurs at the base of the core between 2.6 and 2.7 m (Figure 3). *Brathauer et al.* [2001] recently assessed the calibration of the *C. davisiana* curve with the oxygen isotope stratigraphy. Their records from four core sites in the Atlantic sector of the Southern Ocean show a maximum peak in the relative abundance of *C. davisiana* at the LGM and two or three smaller peaks during the deglacial [*Brathauer et al.*, 2001]. The LGM abundances in the *Brathauer et al.* [2001] records are ∼5% greater than those during the deglacial. The features of the *C. davisiana* curve from KC073 are consistent with those observed by *Brathauer et al.* [2001] adding strength to the inferred chronology.

[12] In addition to the *C. davisiana* biostratigraphic marker, nine AMS radiocarbon dates on bulk organic carbon were obtained for core KC073 (Table 1). KC073 was extracted with good recovery and no evidence of core top disturbance. The core top age (4054 ^{14}C years) is considerably older than the frequently quoted reservoir age for Antarctic marine samples (1200–1400 years) and as such may indicate complex "old" carbon dilution effects [*Stuiver*
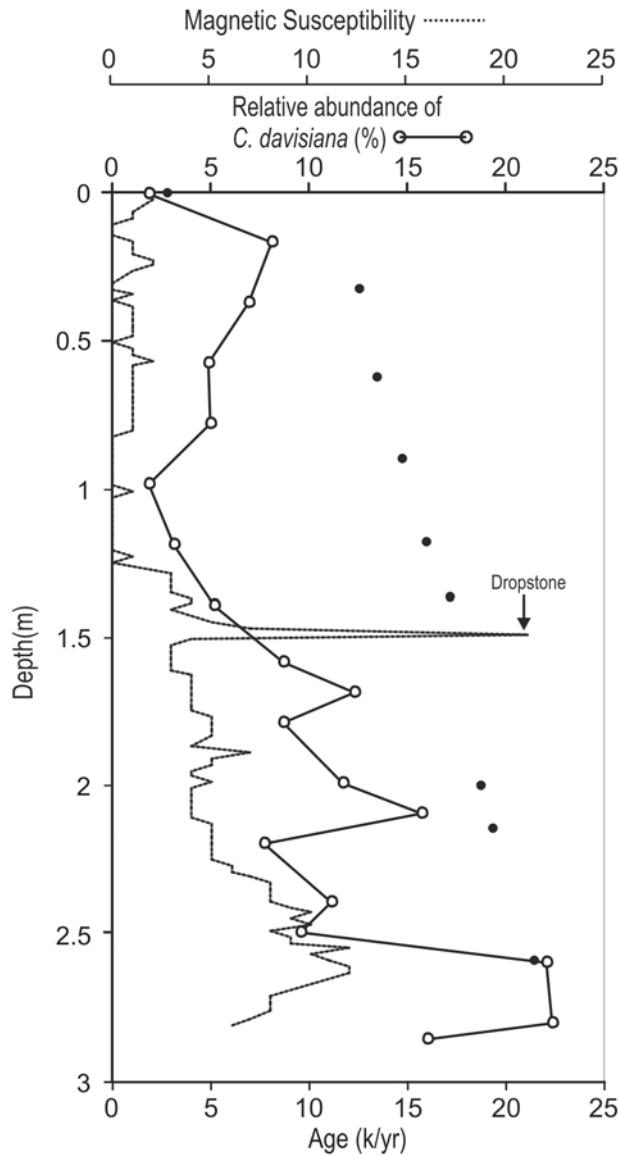
Figure 3. Age-depth plot using calibrated ^{14}C dates (calendar years) (solid circles). Down-core relative abundance of the radiolarian *Cycladophora davisiana* (open circles) and magnetic susceptibility measurements (dotted line) are shown; highest values coincide with the Last Glacial Maximum as described by *Brathauer et al.* [2001], *Hays et al.* [1976], and *Pudsey and Howe* [1998].

and Quay, 1981; *Berkman and Forman*, 1996]. Anomalously old dates from Antarctic marine surface sediments are reported throughout the Antarctic region [*Andrews et al.*, 1999; *Harris*, 2000; *Pudsey and Evans*, 2001]. The total organic carbon in the sediments of KC073 consistently exceeds 0.6%, above the recommended level of >0.4% for reliable AMS dating. The dates are in stratigraphic order and below 0.36 m show an excellent linear correlation (R^2 = 0.9875). Above 0.36 m there is a considerable decrease in the sedimentation rate (Figure 3) which will be discussed in section 5.1. The radiolarian stratigraphy supports the ^{14}C chronology, with both approaches dating the basal sedi-

ments to the LGM. The radiocarbon dates have been converted to calendar years using CALIB4.4 [*Stuiver and Reimer*, 1993; *Stuiver et al.*, 1998] and all dates referred to in the text are calendar years.

[13] Compositional variations in the lithogenic fraction were determined by point counting [*Pudsey*, 1993]. In the upper 0.4 m of the core sand size analysis by sieving was conducted at 2 cm intervals. A 4 cm sampling interval was used for the diatom assemblage data. The sample preparation technique was modified from *Scherer* [1994] and allows quantitative diatom concentrations to be calculated. Taxonomic identification was undertaken on an Olympus BX40 microscope at ×1000 magnification. The assemblage data were compiled from counts of 400–500 valves per sample.

[14] *Chaetoceros* resting spores (CRS) were found to make up over 80% of the assemblage throughout the upper 2.0 m. In order to assess the contributions of the minor species to the overall assemblage, additional counts of approximately 500 individual valves excluding the CRS (*Chaetoceros*-free count) were made. The dominance of CRS throughout the top 2.0 m strongly biases the relative abundance data. Figure 4 clearly shows the bias arising from the inclusion of CRS in the relative abundance. This effect can be alleviated using the *Chaetoceros*-free count data but then the importance of minor taxa is greatly overestimated. The species succession of the CRS-free count data is very different from that of the complete relative abundance data (Figure 4). In order to provide a data set that is not biased by inclusion or exclusion of CRS we calculated absolute numbers for each individual species to provide a set of more independent variables. The absolute numbers were calculated using *Scherer*'s [1994] method of determining quantitative diatom abundance.

4. Assemblage Data

4.1. Diatom Analysis

[15] Diatom distribution is controlled by a combination of environmental parameters including water temperature, salinity and stability as well as light, nutrient availability and sea ice cover [*DeFelice and Wise*, 1981; *Dunbar et al.*, 1985; *Leventer and Dunbar*, 1996; *Zielinski and Gersonde*, 1997; *Cunningham and Leventer*, 1998]. Near to the continent, sea ice, light availability and water column stability are the dominant factors influencing diatom assemblages [*DeFelice and Wise*, 1981]. Beyond the Antarctic coast, temperature, nutrient availability and stratification play an increasingly important role in the distribution and community structure of the diatoms. In addition to environmental controls on the living assemblage in the surface waters, the sedimentary assemblage is influenced by physical effects during transport to the seafloor, including aggregation, dissolution and advection. These alter the speed at which deposition occurs and bias the diatom assemblage preserved in the sediments. Despite these alterations, the diatom record in the sediments reflects the productivity in the surface waters [*Leventer and Dunbar*, 1996; *Zielinski and Gersonde*, 1997].

[16] The core site is situated far north of the controlling influence of modern sea ice cover and the site is in partial

Table 1. Radiocarbon Dates From Bulk Organic Matter in Core KC073

Laboratory Code	Sample	Depth, cm	^{14}C Age, years B.P. ±1σ	Carbon Content, wt %	Calibrated Age Ranges (±1σ)[a]
AA47225	KC073	0–1	4,054 ± 40	1.8	2,622–2,553
OxA12843	KC073	36	12,460 ± 240	-	12,984–12,177
OxA12844	KC073	64	13,100 ± 280	-	14,330–13,278
OxA12845	KC073	88	14,120 ± 180	-	15,294–14,664
OxA12846	KC073	116	14,850 ± 450	-	15,820 ± 580
AA47226	KC073	136–137	15,832 ± 90	0.6	16,950 ± 310
AA47227	KC073	200–201	17,630 ± 100	0.7	19,020 ± 345
AA47228	KC073	208–209	18,060 ± 120	0.7	19,510 ± 360
AA47229	KC073	260–261	20,740 ± 140	0.6	21,935 ± 115

[a]Age corrected using the regional ^{14}C correction age of 1300 years B.P. and calibrated using CALIB 4.4.

daylight all year-round. A strong seasonal temperature effect is still apparent and reflects the northward displacement of surface waters in austral winter. The water temperature is typically ~7°C in summer and ~3°C in winter [*Olbers et al.*, 1992]. Productivity is greatest during the summer months when the Polar Front (PF) is at its most southerly position. Diatom productivity is noted to be highest just south of the PF while carbonate productivity increases northward from the PF [*Burckle and Cirilli*, 1987]. The preservation of diatoms in core KC073 is excellent throughout and suggests that bias from selective dissolution will be minimal.

[17] Diatoms were identified to species and genus level, and groups assigned for principal component analysis. The ecological associations of these species and groups have been determined from previous studies [*Leventer and Dunbar*, 1996; *Armand*, 1997; *Zielinski and Gersonde*, 1997; *Leventer*, 1998; *Armand and Zielinski*, 2001; *Taylor and McMinn*, 2002; *Taylor and Sjunneskog*, 2002]. Changes in the floral assemblage were analyzed by principal component analysis (PCA) using the Multi-Variate Statistical Package (MVSP) [*Kovach*, 1999]. PCA was used to quantify the significance of assemblage variations. Component scores indicate the significance of assemblage variations

between samples. Variable loadings reflect how important a species is at describing the variation within an assemblage. The first few axes of the PCA describe the main patterns of variance in the data. The PCA analysis was carried out on absolute valve numbers calculated from the total and *Chaetoceros* free counts and restricted to species comprising more than 0.5% of the assemblage. A log transformation was applied to down weight the influence of dominant taxa [*Ter Braak and Smilauer*, 2002]. This method of analysis has been shown to divide the assemblage into environmentally significant groups [*Cunningham and Leventer*, 1998].

4.2. Diatom Taxa

4.2.1. *Chaetoceros* Resting Spores

[18] *Chaetoceros* resting spores (CRS) dominate many of the diatom assemblages in sediments of the Antarctic coastal regions with highest abundances found in the sediments of the Antarctic Peninsula region [*Zielinski et al.*, 1998; *Crosta et al.*, 1997]. The relative abundances of diatom species in core KC073 are comparable with those of the Antarctic Peninsula with CRS contributing over 80% to the assemblages in the upper 2 m of the core. *Chaetoceros* is a noted opportunistic genus that forms resting spores when water column conditions limit cell growth. These resting spores are much more
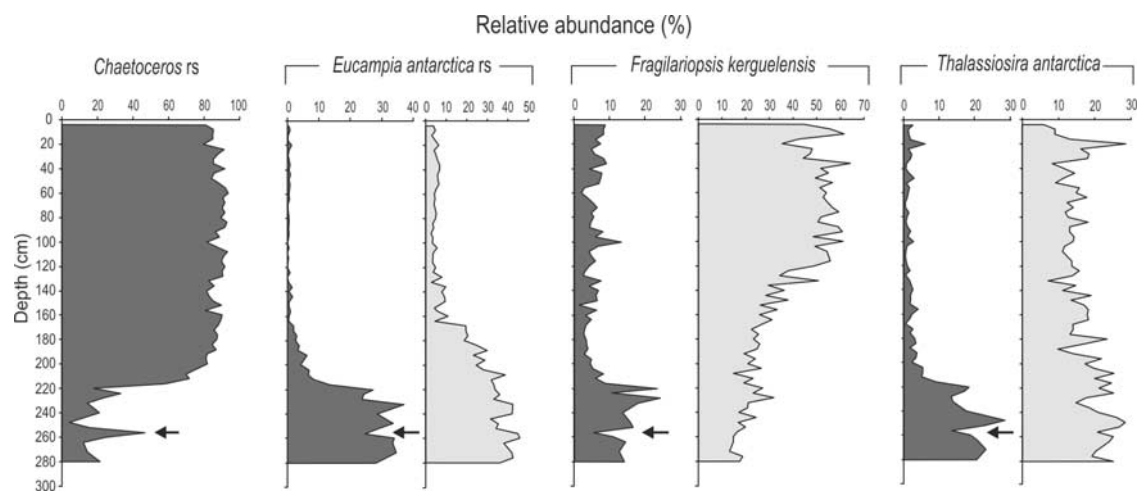

Figure 4. Plots showing difference in relative abundance plots including (dark shading) and excluding (light shading) *Chaetoceros* resting spores (CRS). The bias introduced by the dominance of CRS is evident in the offset of the percentage abundance of the "minor" taxa. The arrows mark out one horizon (260 cm) where the increase of CRS by almost 30% produces a corresponding drop throughout the remainder of the assemblage.

heavily silicified than the vegetative valves and can remain viable as seeds for up to two years [*Crosta et al.*, 1997]. Those that settle to the sediment are resistant to dissolution and are preferentially preserved.

4.2.2. *Eucampia antarctica*:

[19] *Eucampia antarctica* is found throughout Antarctic waters and sediments. *Eucampia antarctica* produces resting stages that are more heavily silicified than the vegetative valves and are preferentially preserved in the sediments. In modern sediments relative abundances of *E. antarctica* rarely exceed 20%, while at the LGM abundances of up to 40% and more in sediment assemblages are found throughout the Southern Ocean [*Burckle and Cooke*, 1983; *Abelmann and Gersonde*, 1988; *Burckle and Burak*, 1988]. No analogues for the relative abundances found in sediments of LGM age are observed in modern sediments. *Shemesh et al.* [1989] suggest that higher concentrations of *E. antarctica* during the LGM are a preservation bias from either a greater production of resting spores associated with unfavorable conditions, or as result of winnowing at the sediment-water interface which would preferentially remove smaller, less robust diatom frustules. Another view is that increased sea ice and iceberg melting sustained a larger *E. antarctica* population during the LGM [*Burckle*, 1984]. The occurrences of *E. antarctica* in modern sediments suggest that its distribution is related to surface waters of the Antarctic zone and the Polar Front Zone (PFZ), and cannot be related directly to sea ice [*Zielinski and Gersonde*, 1997].

4.2.3. *Fragilariopsis kerguelensis*

[20] *Fragilariopsis kerguelensis* commonly dominates open ocean sediment diatom assemblages throughout the Southern Ocean. Despite being present in high concentrations in the sediments, this diatom species is rarely dominant in the water column assemblage. *Fragilariopsis kerguelensis* is a heavily silicified species that exploits water column conditions beyond the sea ice and spreads northward in the Antarctic Surface Water layer. It is associated with the open ocean where maximum abundances of 70–80% are found in sediments between the maximum winter sea ice edge and the PF [*Burckle and Cirilli*, 1987]. Distribution of *F. kerguelensis* is limited by the 0°C isotherm to the south and the PFZ to the north and coincides with the circumpolar diatom ooze belt. Northward displacement of the maximum distribution is limited by the geographic confines of the PFZ [*Burckle and Cirilli*, 1987].

4.2.4. *Fragilariopsis curta* and *Fragilariopsis cylindrus*

[21] Both *Fragilariopsis curta* and *Fragilariopsis cylindrus* are generally restricted to areas south of the PF and have been observed in a range of sea ice environments and in waters closely influenced by sea ice, where they often occur as the dominant species [*Zielinski and Gersonde*, 1997]. *Gersonde and Zielinski* [2000] demonstrate that the abundance of *F. curta* and *F. cylindrus* can be employed as a proxy for winter sea ice extent in the Southern Ocean. The northern boundary of common occurrence (3–15% *F. curta* and 0.3–3% *F. cylindrus*) coincides with the maximum winter sea ice extent. *Fragilariopsis curta* valves are relatively well silicified and preserved, except in areas of severe opal depletion [*Gersonde and Zielinski*, 2000].

4.2.5. *Rhizosolenia* spp

[22] The identifications in this paper follow the descriptions and taxonomy outlined by *Armand and Zielinski* [2001]. *Rhizosolenia antennata* f. *semispina* is the most common species throughout the Southern Ocean and has been documented from open water to coastal sea ice, although its highest abundances correspond to waters of 0.5°–1°C [*Jordan and Pudsey*, 1992; *Zielinski and Gersonde*, 1997; *Crosta et al.*, 1998a]. *Armand and Zielinski* [2001] linked the resting spore of *R. antennata* f. *semispina* (*R. antennata* f. *antennata*) with open ocean waters and not sea ice environments.

4.2.6. *Thalassiosira antarctica*

[23] *Thalassiosira antarctica* is a bipolar diatom that has been noted in high abundances in a variety of oceanographic settings [*Fryxell et al.*, 1981]. In the Antarctic *Thalassiosira* species have traditionally been documented as open ocean species [*Cunningham and Leventer*, 1998]. However, recent studies have recognized that different species respond to different environmental parameters [*Armand*, 1997]. *Thalassiosira antarctica* includes a warm and a cold water form which are morphologically distinct [*Villareal and Fryxell*, 1983]. The warm water form of *T. antarctica* includes the species *T. scotia* as the two species are difficult to distinguish in the light microscope and have been tentatively assimilated into one species [*Armand*, 1997]. Highest abundances of *T. antarctica/T. scotia* have been documented in coastal regions of Antarctica and the Argentine Basin [*Armand*, 1997; *Zielinski and Gersonde*, 1997]. It has been proposed that in the coastal regions *Thalassiosira antarctica* is an autumn bloom species related to sea ice, particularly loose ice crystals [*Cunningham and Leventer*, 1998]. In the Falkland Trough region occurrences of *T. antarctica* are dominated by the warm water variety (*T. antarctica/T. scotia*).

4.2.7. *Thalassiosira lentiginosa*

[24] This species has similar distribution to that of *Fragilariopsis kerguelensis*. Documented as an open ocean species, it has been recorded at its highest abundances just within the maximum winter sea ice extent in the South Atlantic, while its lowest abundances are along the Antarctic Peninsula and within the Ross and Weddell Seas [*Armand*, 1997; *Zielinski and Gersonde*, 1997]. *Thalassiosira lentiginosa* has a more confined temperature range (0°–7°C) than that of *Fragilariopsis kerguelensis* and is primarily found in the PFZ and the permanently open ocean zone, under the axis of the ACC. *Shemesh et al.* [1989] reported that because of the heavy silicification that characterizes *T. lentiginosa*, its relative abundance in sediments can be enriched by selective dissolution.

4.2.8. *Thalassiosira trifulta*

[25] It is suggested that of the *Thalassiosira* species it is *T. trifulta* that occupies the coldest waters and originates closest to the continent [*Armand*, 1997]. *Armand* [1997] presented a distribution plot of several *Thalassiosira* species which exhibited a bimodal distribution with a southerly component associated with a February SST of ~−0.5°C. This cold water distribution has been attributed to *T. trifulta* [*Armand*, 1997]. The valves of *T. trifulta* are heavily silicified and therefore likely to evade dissolution effects.
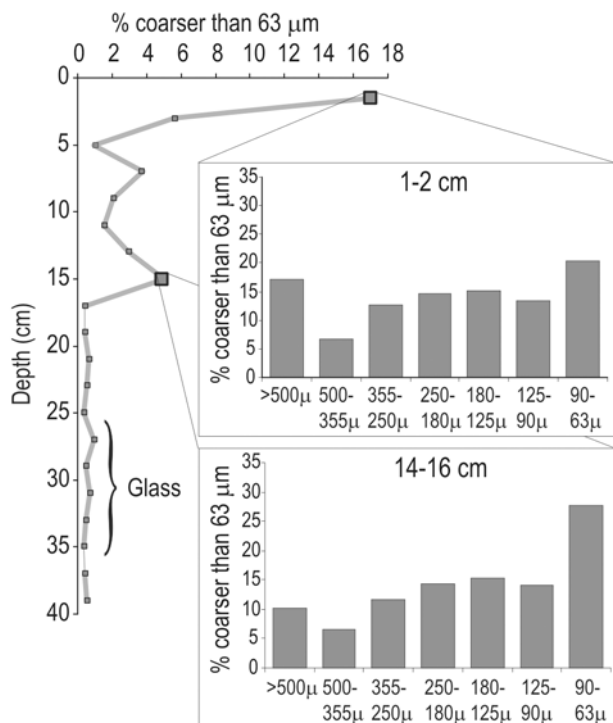
Figure 5. Grain size data for the upper 0.4 m of KC073 showing the coarsening of the surficial sediments.

4.2.9. *Thalassiothrix* Group

[26] This group includes *Thalassiothrix* spp., *Thalassionema nitzschioides* and *Trichotoxon reinboldii*. The geographical distribution of these species remains ambiguous, although *Thalassiothrix antarctica* has been tentatively related to the PFZ and *Thalassiothrix longissima* with the open ocean zone [*DeFelice and Wise*, 1981; *Zielinski and Gersonde*, 1997]. Although individual varieties of *Thalassionema nitzschioides* may relate to localized environmental parameters, the grouped abundance distribution shows an increase north of the winter sea ice edge and a maximum abundance in the sub-Antarctic zone north of the SAF [*Armand*, 1997]. *Trichotoxon reinboldii* are only documented as "abundant around Antarctica" [*Round et al.*, 1990]. In the sediments of KC073 the group consists almost exclusively of *Thalassiothrix antarctica*.

5. Results

5.1. Sedimentation Rates

[27] Sedimentation rates derived from the ^{14}C ages average ~30 cm/kyr below 32 cm. Above 32 cm sedimentation rates slow dramatically. Grain size analysis demonstrates significant coarsening of the sediment above 16 cm and an excess of very fine quartz sand (Figure 5). Below 16 cm the proportion of terrigenous sand is consistently less than 1%. Sand content increases dramatically above 16 cm to a high of ~17% at 1–2 cm, it is poorly sorted and predominantly quartz, with lithic grains including sedimentary, igneous and metamorphic rocks from the Antarctic Peninsula. The presence of grains up to several millimeters across points

to deposition by iceberg rafting, while the excess of very fine quartz sand may result from current winnowing.

[28] The grain size data suggest that the change in sedimentation occurs at 16 cmbsf. If sedimentation rates averaging 30 cm/kyr were maintained up to 16 cmbsf where the sand concentration increases, the sedimentation rates must have declined to ~2 cm/kyr above 16 cmbsf.

[29] Another possible explanation for the apparent change in sedimentation rate in the top 16 cm of the core is loss of sediment during coring. Loss of surficial sediment is a risk with all coring processes. However, although the macrofabric of the sediments can usually be used to determine coring disturbances there is no evidence of a hiatus or coring disruption in the sediments of KC073. Also, it is hard to reconcile the surface age of 2590 years if all the Holocene sediments of KC073 were lost during the coring process. *Skinner and McCave* [2003] suggest that repenetration is the most likely coring problem with Kasten corers and that essentially intact sediments should be recovered down to ~3 m penetration.

[30] From the evidence available it seems most likely that current velocities have inhibited sediment deposition and may have been strong enough to winnow the surface sediments away. This explanation is consistent with the chronology and supported by the grain size data (Figure 5). It is also worthy of note that between 36 and 26 cm common volcanic glass grains in the sand fraction may represent the early Holocene ash layer documented farther south in the Scotia Sea by *Moreton* [1999].

5.2. Valve Concentrations

[31] The depth profile of the total diatom valve concentrations follows a broad decline, which parallels changes in sediment composition from diatom ooze to mud-bearing diatom ooze (Figure 6). Other siliceous microfossils such as radiolarians and silicoflagellates are present as minor components of the sediment throughout the core. As the sedimentation rates below 0.36 m are essentially linear, it is the relative inputs of terrigenous and biogenic sediment to the seafloor that vary, with the total accumulation at the seafloor changing very little.

[32] Diatoms comprise between 80% and 98% of the sediment in the upper 2.00 m and less than 55% in the bottom 0.8 m. The upper 1.2 m contains the highest concentrations of valves in the sediment and is also characterized by the greatest variability in concentrations. Between 1.4 m and 1.7 m concentrations fall to below 8×10^8 valves per gram of dry sediment (v/gds) then rise to $>1.4 \times 10^9$ v/gds at 1.84 m before a gradual decline to $<3 \times 10^8$ v/gds at 2.2 m. Valve concentrations in the bottom 0.6 m of the core are consistently lower than 3×10^8 v/gds.

5.3. Diatom Assemblages

[33] Down-core variations in species assemblage are pronounced (Figure 7). In the upper part of the core the assemblage is dominated by CRS with over 5×10^8 v/gds throughout most of the upper 2 m. *Fragilariopsis kerguelensis, Thalassiosira lentiginosa* and *Thalassiosira antarctica* are also abundant in the upper section of the core. The decline in the contribution of CRS to the assemblage is the most notable feature of the assemblage
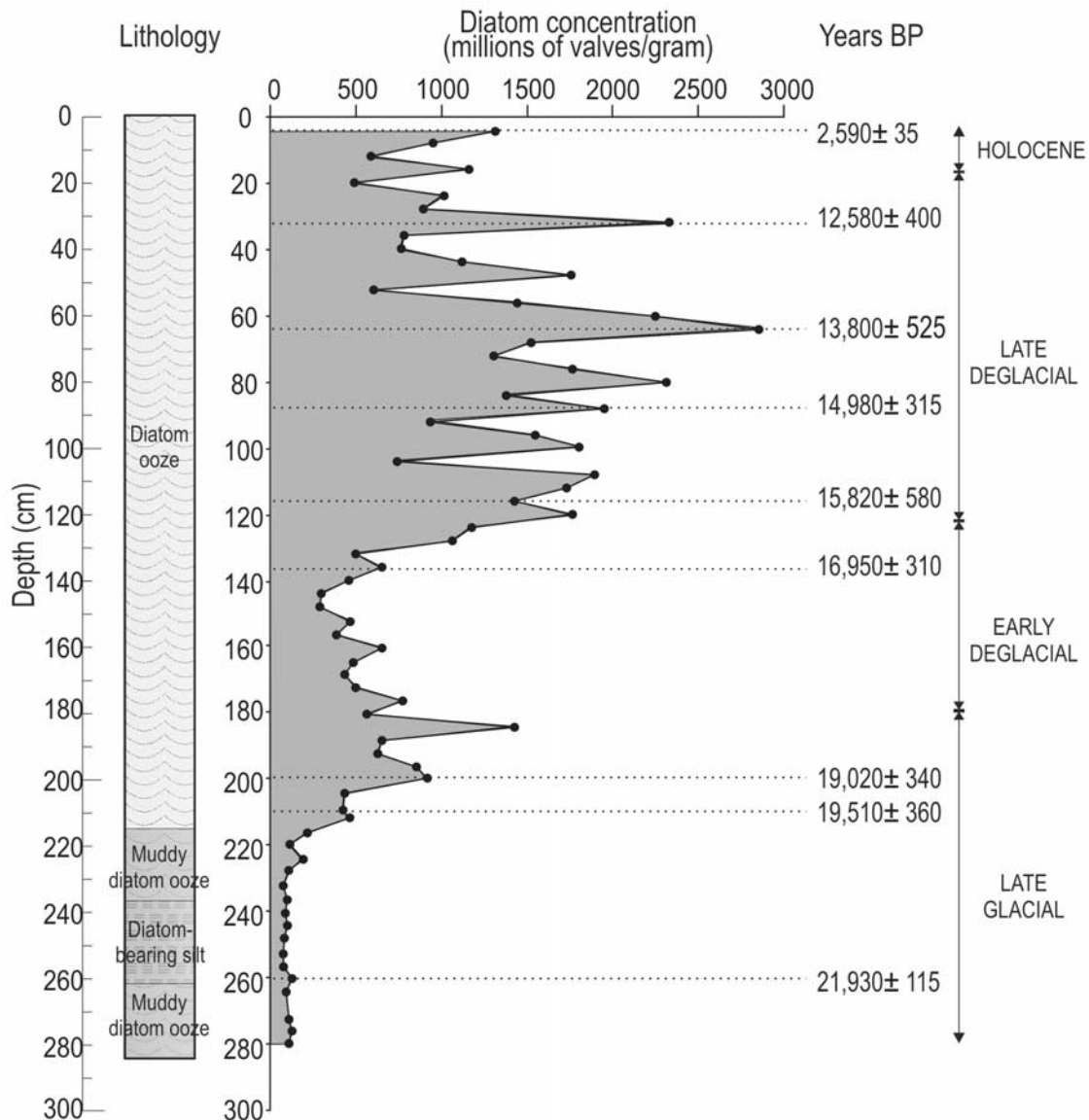
Figure 6. Sediment log and diatom valve concentrations of core KC073 with dates (calendar years) marked.

change, with a drop to <1 × 10^8 v/gds between 2.2 and 2.8 m (Figure 7). *Fragilariopsis kerguelensis, Thalassiosira lentiginosa,* and *Thalassiothrix* group parallel this decline down core, while *Thalassiosira antarctica* remains relatively high throughout the core.

[34] The lower part of the core is characterized by lower abundances of CRS and high abundances of *Eucampia antarctica, Fragilariopsis curta* and *F. cylindrus.* The transition between these two assemblages occurs between 1.5 and 2.1 m. This intermediate interval has the highest relative abundances of *Rhizosolenia* spp. and *Thalassiothrix* group.

5.4. Principal Component Analysis

[35] Wherever possible the genera *Rhizosolenia, Thalassiosira* and *Fragilariopsis* were identified to species level.

Where identification to species level was not possible the valve counts were assimilated in a generic group. Individual species groups with lower than 0.5% abundance were also added to their respective generic group before principal component analysis was carried out.

[36] The principal component analysis (PCA) on the log-transformed data set explains 68% of the total variance within the first three axes. Figures 8a and 8b show the variable (species) loadings for first three axes identified by the PCA and Figure 9 shows the down-core component (sample) loadings for each of the axes.

[37] Axis 1 explains 47.9% of the variance with CRS having the highest loading (Figure 8a). *Fragilariopsis kerguelensis, Thalassiothrix* group, *Rhizosolenia* spp. and *T. lentiginosa* also have significant positive loadings on axis 1 (Figure 8a). *Eucampia antarctica* resting spore (rs) was
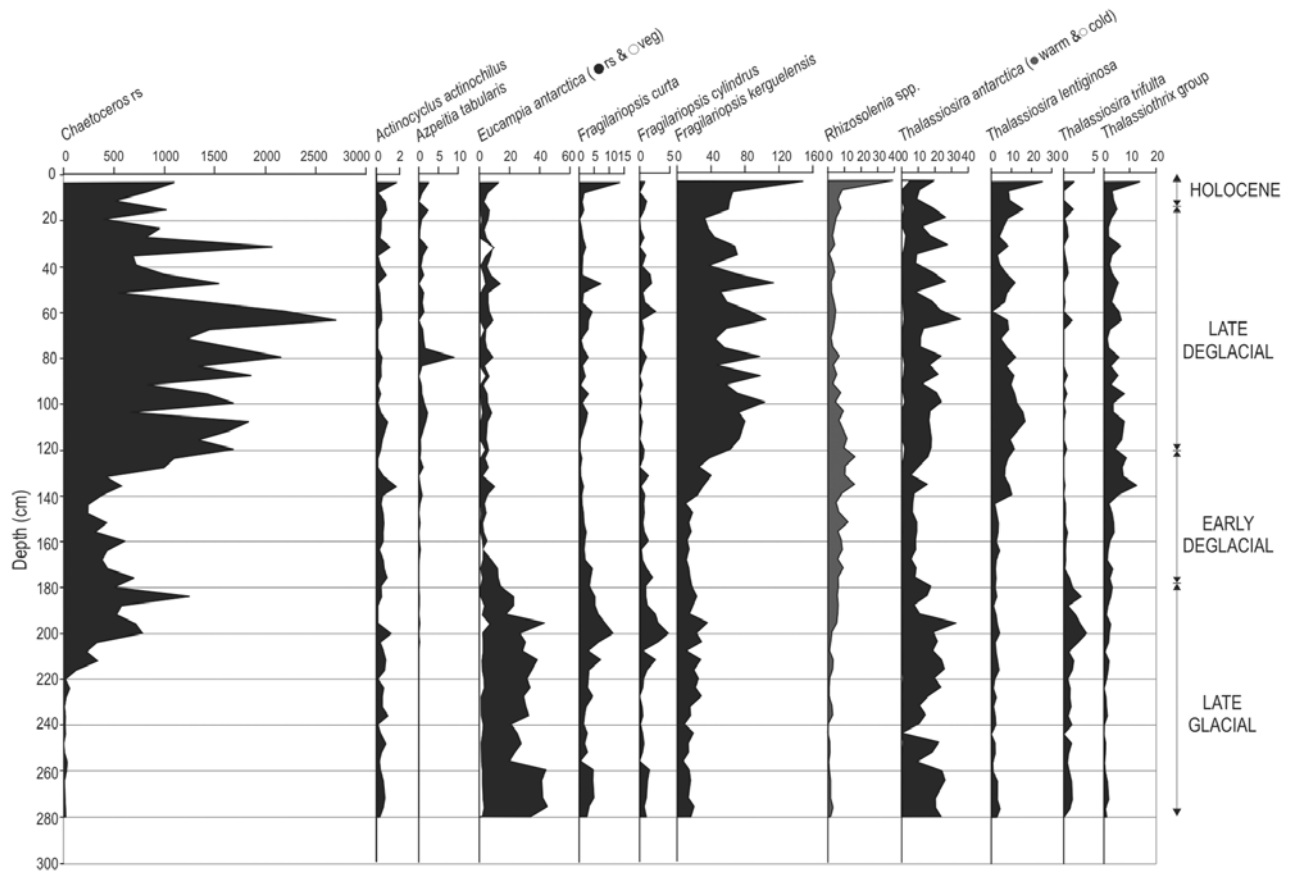
Figure 7. Diatom log for core KC073 showing absolute valve numbers (in millions of valves per gram of dry sediment) for taxa discussed in the text. Values for CRS are calculated from the total count data; all others are calculated from the *Chaetoceros*-free count.

the only variable with significant negative loadings on the first axis. Figure 9 shows the down-core variations in loadings for the axes identified by the principal component analysis. Samples with a high positive component score for axis 1 occur in the top 1.4 m of the core and high negative loadings occur below 2.0 m (Figure 9).

[38] Axis 2 explains 12.6% of the total variance but has no significant positive loadings. The highest negative loadings are for *E. antarctica* rs. In order of rank, *Fragilariopsis curta*, *Thalassiosira antarctica* (warm), *F. obliquecostata*, *F. kerguelensis* and *Fragilariopsis* spp. are the other species with significant negative loadings on axis 2. The majority of samples with high negative component scores on axis 2 occur between 1.8 m and the bottom of the core. However, the highest negative component scores on this axis occur within the top 1.0 m where sharp and high-amplitude shifts between positive and negative component scores occur. The high negative scores at 0.04, 0.16, 0.32, 0.48, 0.64 and 0.80 m, correlate with the more subtle positive peaks evident in axis 1 (Figure 9).

[39] The significant species of axis 2 are indicative of both sea ice conditions (*Fragilariopsis curta*, *F. oblique-costata* and *E. antarctica*) and open ocean conditions (*Fragilariopsis kerguelensis* and *Thalassiosira antarctica*). The two sections of the core with negative component

scores probably reflect two periods when these different conditions prevailed. The lower section of the core with negative component scores on axis 2 (below 1.8 m) corresponds to an assemblage with high absolute abundances of the sea ice species and as such *F. curta*, *F. obliquecostata* and *E. antarctica* are likely to exert the main influence on the component scores below 1.8 m. In the upper core where the high-amplitude variations in component scores occur it is more likely that the component scores are being driven by *F. kerguelensis* and *Thalassiosira antarctica* that both have high absolute abundances in this section of the core.

[40] Axis 3 describes only 7.5% of the total variance. Samples that have high positive loadings for axis 3 lie in the top 1.4 m of the core and below 2.2 m. Negative loadings are predominantly between 1.5 and 2.2 m (Figure 9). Significant positive loadings occur only for *T. lentiginosa* and *F. kerguelensis*. The taxa with significant negative loadings include *Chaetoceros* rs, *F. cylindrus* and *F. curta* (Figure 8b).

6. Discussion

[41] Sediments in core KC073 reflect changes in ocean conditions in the Falkland Trough since the LGM. The record of the late glacial and deglaciation are high resolu-

tion but the Holocene record is incomplete. The chronology is based on the reservoir corrected ^{14}C ages shown in Table 1 and supported by the biostratigraphy of the *C. davisiana* curve (section 3, Figure 5). The palaeoceanographic record can be divided into four distinct episodes: the late glacial (22.5 ka to 18 ka), early deglaciation (18 ka to 16.5 ka), late deglaciation (16.5 to 12 ka) and the Holocene (<12 ka). The late glacial, early deglaciation and late deglaciation episodes are broadly picked out by the PCA results with the negative scores on axis 1 between 2.0 m and 2.8 m characterizing the late glacial; the negative score of axis 3 characterizing the early period of deglaciation and the positive scores of axis 1 correlating with the late deglaciation. Axis 2 highlights the dramatic productivity cycles of the late deglaciation between 0.3 and 1.1 m. The Holocene sediments (younger than 12 ka) are characterized by very low sedimentation rates and increased sand content.

6.1. Late Glacial (22.5 to 18 ka)

[42] Sediment deposition during the late glacial was characterized by low biogenic input and increased terrigenous sediment supply. The diatom assemblage is dominated by species associated with near freezing waters and sea ice including *Fragilariopsis curta* and *F. cylindrus* (Figure 7). *Eucampia antarctica* is most abundant during the late glacial. Axis 1 of the PCA, which dominates from 2.8 m to 2.0 m (~22.5 to 19 ka), demonstrates the importance of *E. antarctica* in the assemblage as it is the only variable with significant negative loading. As there is no modern analogue for *E. antarctica* it is difficult to interpret the significance of the high abundances although it is likely that *E. antarctica* also reflects lower sea surface temperatures (SST) and more abundant ice (potentially ice bergs [*Burckle*, 1984]).

[43] The peak in the absolute numbers of sea ice taxa (*Fragilariopsis curta* and *Fragilariopsis cylindrus*) occurs at 2.0 m (~19 ka). The maximum abundance of *Thalassiosira trifulta* parallels the sea ice taxa abundance maximum, supporting *Armand*'s [1997] suggestion that *T. trifulta* is a cold water taxon. The maximum abundance of sea ice diatoms in the cores also coincides with the initial increase in biogenic deposition following the late glacial, and is likely to represent the period where the core site was close to the winter sea ice limit which is typically associated with higher productivity [*Burckle and Cirilli*, 1987]. The importance of the sea ice taxa in the diatom assemblage at the end of the late glacial period is reflected in the high negative loadings of axis 2 between 2.3 m and 1.7 m (~20 to 18 ka).

[44] *Gersonde and Zielinski*'s [2000] sea ice proxy, on the basis of the relative abundance of *F. curta* and *F. cylindrus*, states that combined abundances of >3.0% are indicative of the average cover of winter sea ice. Average summer sea ice extent is indicated by a drop in biogenic sedimentation and a >3.0% abundance of *F. obliquecostata*. In KC073, *F. curta* and *F. cylindrus* reach their maximum relative abundance at 2.28 m (~20 ka) and have a combined abundance of >3.0% between 2.80 and 2.08 m (~22.5 to 19.5 ka) (Figure 10). Biogenic input was low during this period, and the relative abundance of *F. obliquecostata* frequently exceeds 1% which implies that sea ice may have intermittently lasted through the spring and summer. The fluctuations in the
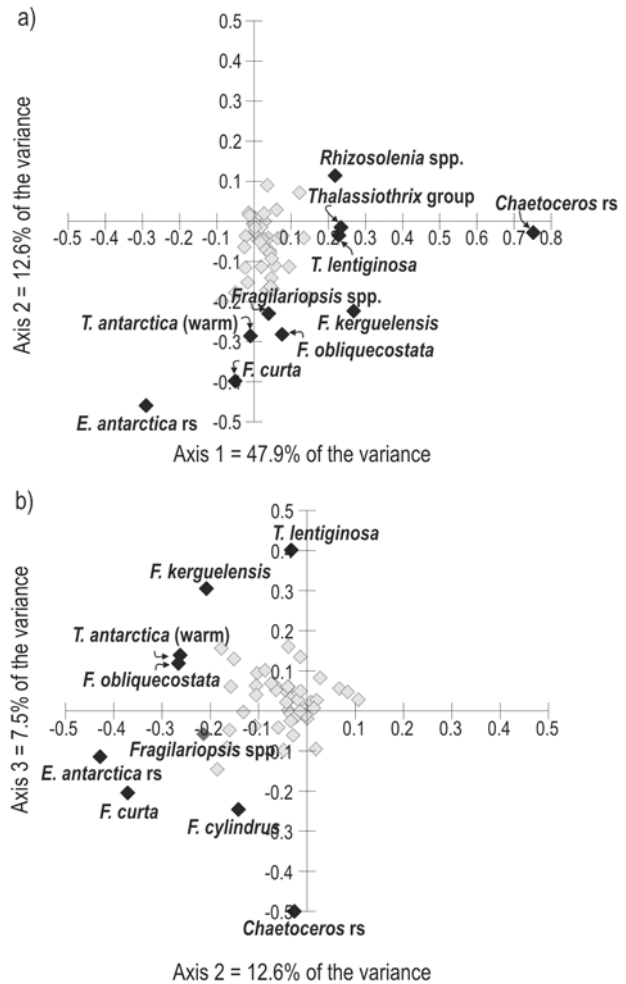

Figure 8. Principal component analysis variable loadings (a) axes 1 and 2 and (b) axes 2 and 3. All variables with loadings of >0.2 on one or more axis are shaded. Species discussed in the text are labeled on each of the plots.

relative abundance of *F. curta*, *F. cylindrus* and *F. obliquecostata* in core KC073 reflect variations in the mean annual duration of sea ice. On the basis of *Gersonde and Zielinski*'s [2000] proxy, we propose that the site of core KC073 was covered by seasonal sea ice during the late glacial. This is an important result as it demonstrates that the winter sea ice limit was at least 5° farther north during the late glacial than at present in the eastern Scotia Sea (Figure 11a). This correlates with previous reconstructions of LGM sea ice extent [*Crosta et al.*, 1998a, 1998b; *Gersonde and Zielinski*, 2000; *Shemesh et al.*, 2002; *Gersonde et al.*, 2003] and suggests that the passage of the ACC and storm tracks through Drake Passage and the Scotia Sea did not preclude sea ice formation in the Falkland Trough. The low concentrations of taxa relating to the PF and sub-Antarctic waters demonstrate that the PF was well north of the site during this period, preventing incursions of sub-Antarctic waters (Figure 11a).

[45] The retreat of maximum sea ice extent at ~19.2 ka reflects the timing of deglaciation of the Antarctic continent, which began its warming trend earlier than in the Northern
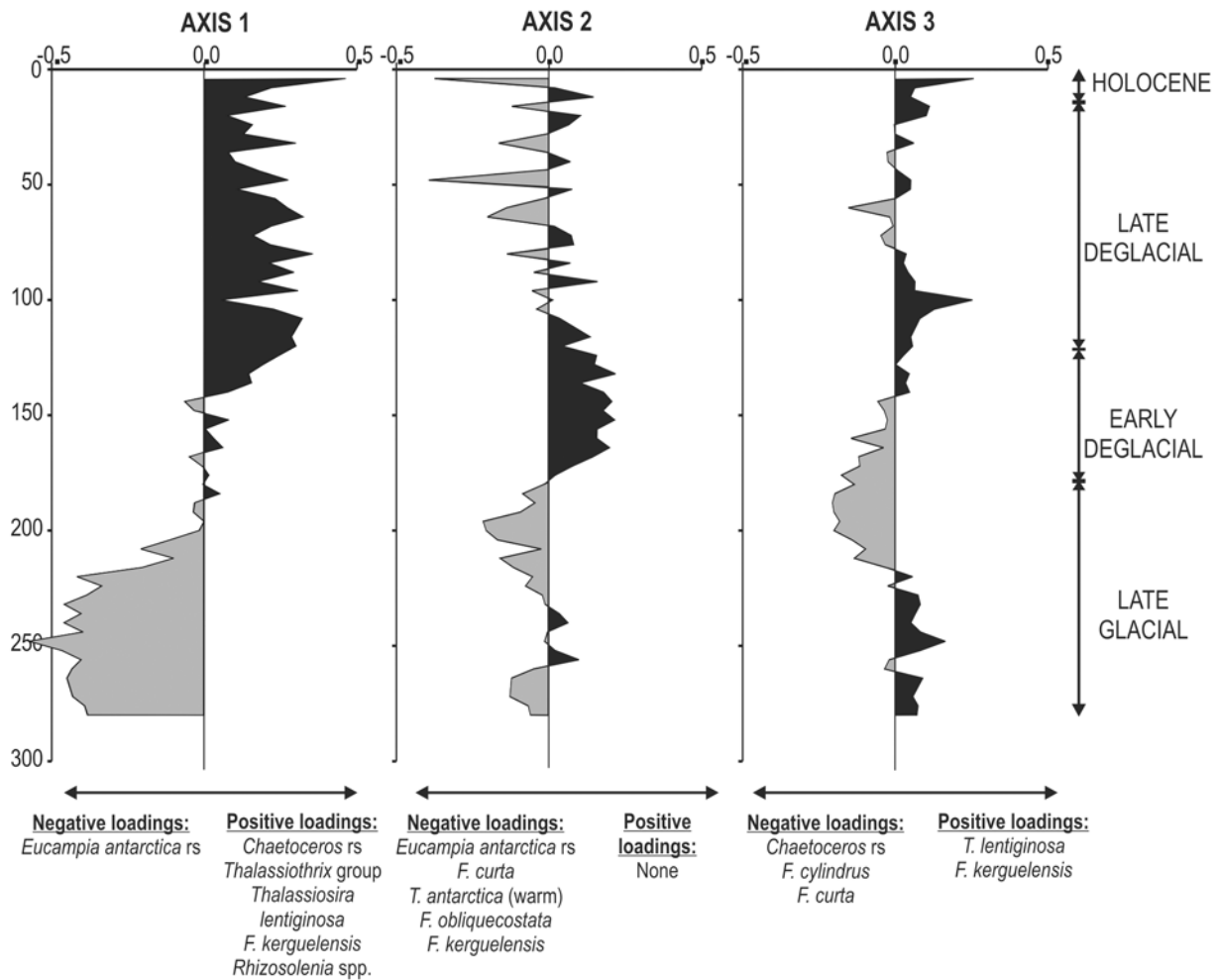
Figure 9. Axes component scores derived from principal component analysis on the absolute abundance data of core KC073. Dark shaded regions denote positive component scores. Variable loadings are marked below to indicate which species influence the variability on the different axes (see Figure 8).

Hemisphere [*Jouzel et al.*, 1995, 2001; *Delmonte et al.*, 2002] and correlates with the timing of sea ice retreat in the eastern Atlantic basin [*Shemesh et al.*, 2002]. *Shemesh et al.* [2002] showed that sea ice extent started decreasing at 19 ka and preceded the increase of atmospheric CO_2 (as recorded in ice cores) by approximately 2000 years.

6.2. Early Deglacial (18 to 16.5 ka)

[46] Total valve concentration and CRS numbers increase abruptly at the top of the glacial interval and mark the beginning of deglaciation. The initial increase in biogenic flux is consistent with a location associated with the maximum winter sea ice limit [*Gersonde and Zielinski*, 2000]. The cold water and sea ice species that characterize the late glacial period gradually decline between 2.0 m and 1.7 m (~19 to 18 ka) and are replaced in the assemblage by *Rhizosolenia* spp. and the *Thalassiothrix* group (Figure 7). The shift away from a diatom assemblage dominated by sea ice taxa to one dominated by *Rhizosolenia* and *Thalassiothrix* group is demonstrated in the PCA by the shift from negative to positive component scores on axis 2 (Figures 8

and 9). The rise in *Rhizosolenia* spp. and the *Thalassiothrix* group coincides with a period of reduced productivity between 1.7 m and 1.3 m (~18 to 16.5 ka) (Figure 6). This may be explained by continuing retreat of sea ice out
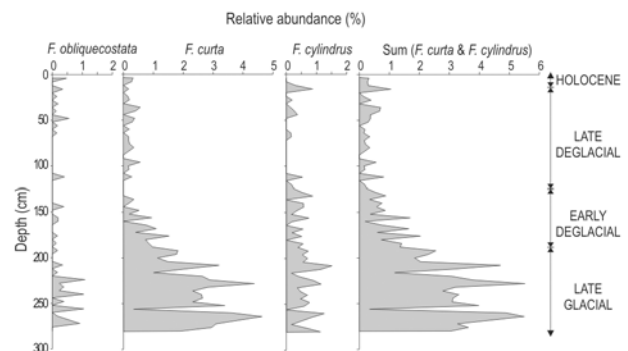

Figure 10. Relative abundance plots of sea ice indicator species, *Fragilariopsis obliquecostata*, *F. curta*, and *F. cylindrus*.
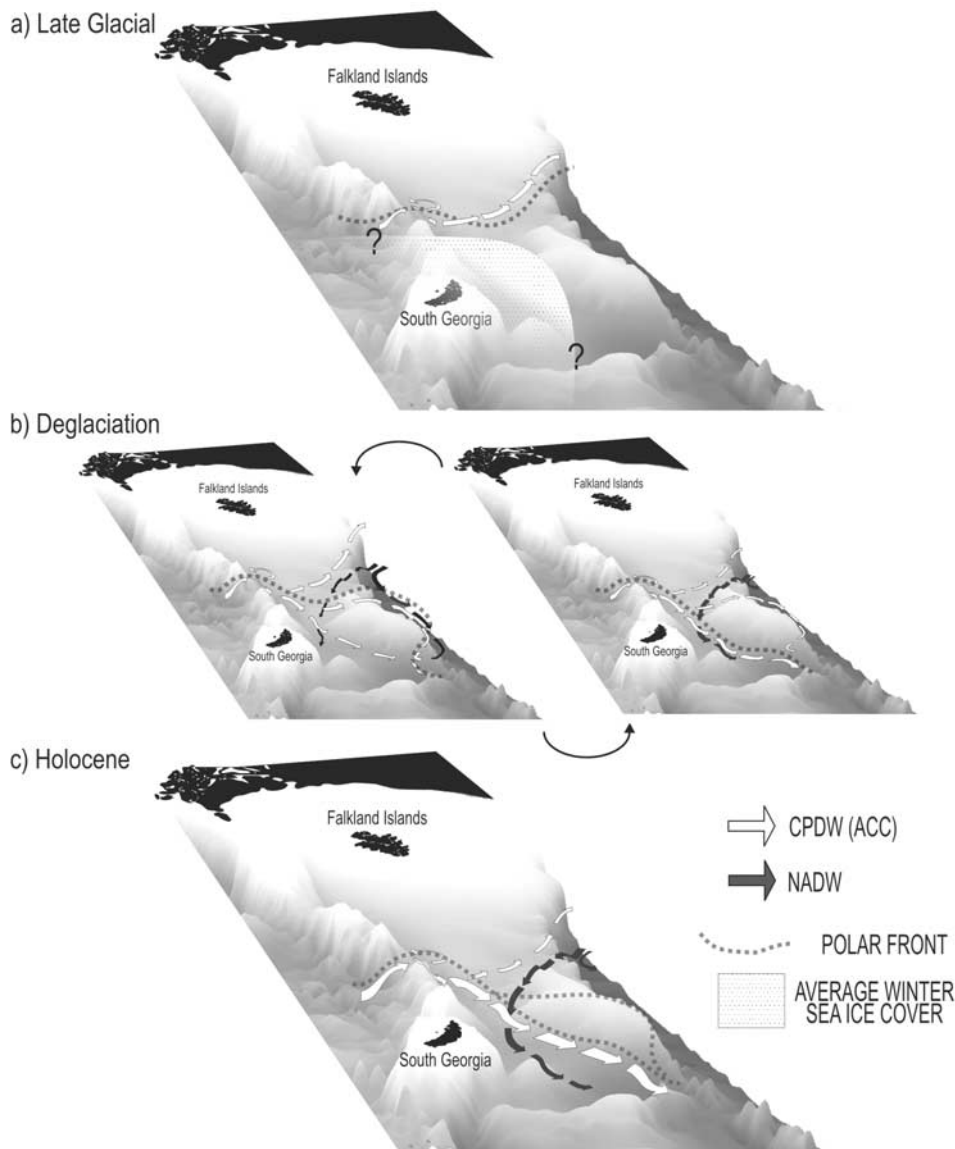
Figure 11. Schematic of oceanographic conditions in the Falkland Trough: (a) late glacial, circulation dominated by northward displacement of the Polar Front and Antarctic Circumpolar Current (ACC), sediments with increased terrigenous input (IRD), and low diatom productivity dominated by cold water and sea ice taxa; (b) deglaciation, productivity cycles in sediments driven by strengthening and weakening of Atlantic Deep Water (NADW) over flow, carrying *Thalassiosira antarctica* and *Chaetoceros* resting spores (CRS) from the Argentine Basin and Falkland Plateau; and (c) Holocene, deposition inhibited by the strength of the ACC flow through the Falkland Trough, sediments characterized by increased sand content. CPDW is Circumpolar Deep Water. See color version of this figure in the HTML.

of the area, as regions beyond the sea ice margin experience decreased productivity and flux [*Zielinski and Gersonde*, 1997]. The decline in the contribution of sea ice taxa to the assemblage supports this interpretation also.

[47] The axis 2 assemblage is difficult to interpret, given the ambiguity concerning controls on the modern distribution of *Rhizosolenia* spp. and *Thalassiothrix* group species. The abundance of both groups increases gradually from the sea ice maximum identified at 2.0 m (19 ka) to a peak at

1.38 m (16.9 ka). The common feature in their modern distribution is of a general increase away from the sea ice maximum. *Rhizosolenia* spp. may also respond favorably to increased fresh water (meltwater) flux within the surface waters, given its response to fluvial outwash in temperate regions [*Malej et al.*, 1995]. *Thalassiothrix antarctica* is the most common of the *Thalassiothrix* group in the sediments of KC073 and as such the main signal is likely to relate to this species. However, the controls on the modern distribu-

tion of *Thalassiothrix antarctica* remain poorly constrained. *Thalassiothrix antarctica* has been tentatively linked with the polar front (PF) but there are few published data to support this [*Smetacek et al.*, 2002; *Tremblay et al.*, 2002].

[48] The gradual increase in the abundance of *Rhizosolenia* and *Thalassiothrix* group taxa from 2.0 m to 1.38 m (~19 to 16.9 ka) fits well with what is known about their modern ecology and demonstrates an increasingly distal sea ice margin. Given the proximity of the KC073 core site to the bifurcation of the PF (Figure 1) it is likely that ocean conditions are sensitive to variations in the mainstreaming of the ACC and PF either side of the Maurice Ewing Bank (Figure 2) as described by *Arhan et al.* [2002]. If high abundance of *Thalassiothrix antarctica* is a proxy for the PF then it suggests that the PF was closest to the site at this time. However, the record of *Fragilariopsis kerguelensis*, a recognized proxy for the main current flow of the ACC (which is noted to underlie the PF), suggests otherwise. The abundance of *F. kerguelensis* rises through the upper section of the deglacial but only reaches its first peak at 1.0 m (~15.2 ka). If the PF and main ACC flow are closely linked, then the *F. kerguelensis* data suggest that the main axis of the ACC and the PF remained distal until ~15.2 ka. *Thalassiosira lentiginosa* is also a proxy for open ocean conditions and the ACC, and this species increases in parallel with *F. kerguelensis* supporting the latter interpretation.

[49] The meaning of the correlative peaks in *Thalassiothrix* group/*Rhizosolenia* species remains elusive, but the evidence in this core suggests that the abundance peaks in these taxa do not relate directly to the PF. A further indication that the PF had not migrated this far south by 16.9 ka (1.38 m) is the reduced biogenic flux. The PF is associated with increased primary productivity, which is classically reflected in the sediments by a greater biogenic flux. Between 1.7 m and 1.3 m (~18.0 to 16.5 ka) the diatom valve concentrations are reduced. This could be due to diminished primary productivity, winnowing or dissolution. We interpret the drop in valve concentrations as a fall in primary productivity in the overlying waters as there is no evidence of dissolution or winnowing: Lightly silicified diatoms are still preserved; species diversity remains fairly constant throughout the core; there is no preferential removal of easily entrained diatoms; and there is no evidence of hiatuses or structures in the sediment fabric that would indicate sediment disturbance.

[50] The diatom record suggests an open ocean environment between the PF and the sea ice edge where reduced biogenic content is likely to be the result of reduced primary productivity. Lower primary productivity is a characteristic of the permanently open ocean zone between the PF and the sea ice edge [*Zielinski and Gersonde*, 1997]. This interval of reduced biogenic flux and relatively consistent diatom assemblage between 1.7 m and 1.3 m suggests that the open ocean conditions prevailed between ~18.0 and 16.5 ka.

[51] The subsequent rise in valve concentrations from >300 × 10^6 v/gds at 1.38 m (~16.9 ka) to >1800 × 10^6 v/gds at 1.08 m (~15.5 ka BP) reflects the increase in CRS, *Fragilariopsis kerguelensis* and *Thalassiosira lentigi-*

nosa. *Fragilariopsis kerguelensis* and *T. lentiginosa* document the growing influence of the ACC and Polar Front on the site and the shift to an assemblage dominated by axis 1.

6.3. Late Deglacial (16.5 to 12.0 ka)

[52] The dominance of *Fragilariopsis kerguelensis* and *Thalassiosira lentiginosa* is consistent with the modern ACC assemblage preserved in the sediments. The concentrations of CRS (500 × 10^6 to 2700 × 10^6 v/gds) are comparable with those observed off the Antarctic Peninsula and very unusual for the open ocean environment in Antarctica [*Crosta et al.*, 1997]. The concentrations are too high to be a result purely of advection from distal production sites and suggest a local source. CRS, *F. kerguelensis*, *T. lentiginosa* and *T. antarctica* exhibit highly variable abundances throughout the late deglaciation. The overall valve concentration in the sediments reflects these variations. The frequency of these fluctuations is submillennial with individual peak and trough durations of 200 to 300 years. Many of the peaks and troughs include more than one sample validating the signal of the variability.

[53] The PF migration into the Falkland Trough has been placed at the 1.0 m horizon (~15.2 ka) where the ACC indicator species (*Fragilariopsis kerguelensis* and *Thalassiosira lentiginosa*) reach their first significant peak. The rapid fluctuations in the numbers of diatom cells preserved in the sediment begin at this horizon. Several mechanisms can be invoked to explain this pattern of sedimentation: (1) changes in the primary productivity at the site; (2) changes in the aggregation and transport of the frustules to the sediment surface; (3) changes in the preservation in the sediment through either dissolution or winnowing; and (4) dilution of the diatom concentrations by increased terrigenous deposition.

[54] Dissolution events would preferentially remove smaller and the more lightly silicified diatom frustules from the assemblage, for which there is no evidence. Dilution by terrigenous sediments could explain the pattern of sedimentation observed in KC073 between 1.0 m and 0.16 m (~15.2 ka and 12.0 ka). However, there are no obvious changes in the sediment composition during this interval. Irrespective of whether the variations in valve concentration are driven by terrigenous or biogenic fluxes the pattern is significant as it indicates rapid oceanographic change. Submillennial changes in oceanographic conditions are commonly observed in other regions of Antarctica [*Domack et al.*, 1993; *Leventer et al.*, 1996]. Given the paucity of evidence for dissolution or dilution by terrigenous material, changes in primary productivity or transport to and from the sediment appear the most credible explanations for the observed patterns of sedimentation.

[55] *Crosta et al.* [1997] advocate that CRS in sediments of the SW Atlantic are a product of transport via the ACC from the northern Antarctic Peninsula. Several authors have found evidence of productivity cycles in the northern peninsula region also [*Domack et al.*, 1993; *Leventer et al.*, 1996]. However, there are several problems with trying to explain the diatom record of KC073 using a Peninsula source and ACC transport mechanism. First,

much of the inner shelf of the peninsula remained glaciated until at least ~13 ka [*Anderson*, 1999; *Domack et al.*, 2001]. Although the northern peninsula was probably deglaciated earlier, it is hard to envisage that the productivity patterns were the same as during the Holocene. *Crosta et al.*'s [1997] schematic showed CRS concentrations decreasing with distance from the source. This does not fit with the pattern seen in the Falkland Trough. In KC073 CRS concentrations are comparable with the northern Peninsula region while in the Scotia Sea and western Falkland Trough concentrations are consistently lower [*Allen*, 2003].

[56] *Zielinski and Gersonde* [1997] record high concentrations of CRS in sediments of the Argentine Basin. They suggest the CRS found in the Argentine Basin are transported by UCPDW from a high productivity region over the Falkland Plateau. The proximity of the PF would directly affect the primary productivity of the region while the strength in the flow of water masses would strongly influence the settling regime of the diatoms in the water column and at the sediment surface. The Falkland Plateau is the only documented, local, high-productivity site of CRS and could be the source of the CRS in KC073. The Falkland Plateau lies to the northwest of the core site and the only southeasterly flowing water mass that could transport CRS from the Falkland Plateau to the mouth of the Trough is NADW (Figure 2). NADW overflow into the Falkland Trough would provide a source of entrainment for diatoms sinking out from the surface waters and transport them into the eastern Falkland Trough. Shifts in the position of the polar front and the main flow of the ACC over the Falkland Plateau would impact on the southerly flow of NADW and prompt variations in the strength of NADW overflow (Figure 11b). Given that there is scope within the present oceanographic setting for episodic changes in the strength and position of the PF and the corresponding NADW and ACC flow [*Arhan et al.*, 2002], it is proposed here that the rapid shifts in diatom valve concentrations indicate similar internal dynamics active within this region during the late deglacial. It is proposed that strong overflow of NADW entrained high numbers of CRS over the Falkland Plateau and carried them southeastward into the Falkland Trough (Figure 11b). The variation in the concentration of CRS in the sediments thus reflects the strength of the NADW overflow into the Falkland Trough.

[57] *Fragiliariopsis kerguelensis* and *Thalassiosira antarctica* (warm) also exhibit high-frequency abundance fluctuations between 1.0 m and 0.16 m (~15.2 and 12 ka). The importance of these species on the assemblage variations is demonstrated by their high negative loadings on axis 2 and the high-amplitude changes from positive to negative component scores of axis 2 revealed by the PCA. The contribution of *T. antarctica* is particularly noteworthy as this species has only been observed in high abundances in coastal regions of Antarctica and in the Argentine Basin as *T. scotia* [*Armand*, 1997; *Zielinski and Gersonde*, 1997]. Its presence in KC073 supports the theory that the assemblage composition is being driven by influx of NADW from the north, bringing populations of *T. antarctica* and

Chaetoceros spp. from the Argentine Basin and Falkland Plateau into the Falkland Trough.

[58] The North Atlantic influence on this sector of the Southern Ocean has been suggested by coupled ocean-atmosphere general circulation models [*Ninnemann et al.*, 1999; *Schmittner et al.*, 2003] and inferred to explain submillennial-scale glacier fluctuations during the Holocene on South Georgia [*Rosqvist and Schuber*, 2003]. The record of KC073 suggests that the South Atlantic sector was influenced by NADW during deglaciation. This result is significant as it shows that the onset of NADW overturning impacted on the Southern Ocean during deglaciation. Our interpretation supports the work of *Piotrowski et al.* [2004], who document the arrival of NADW in the SE Atlantic by 17.1 ka and supports other Southern Hemisphere studies that advocate episodic North Atlantic–driven climate signals [*Andres et al.*, 2003; *Pahnke et al.*, 2003; *Rosqvist and Schuber*, 2003; *Schmittner et al.*, 2003].

6.4. Holocene (12 ka−)

[59] The greatly reduced sedimentation rate during the Holocene reflects a dramatic change in the depositional environment at the core site. We propose that the reduction is related to the current velocities over the site (section 5.1). The ACC is a strong current which is known to scour sediments from the seafloor where flow is constrained, such as in Drake Passage [*Pudsey and Howe*, 1998]. The evidence suggests that ACC flow over the site has been stronger during the Holocene than during the late glacial and deglaciation where the sediments remained undisturbed. The diatom assemblage only shows a significant change above 8 cm where there is a noticeable rise in the abundances of *Fragilariopsis curta*, *F. kerguelensis*, *Rhizosolenia* spp. and *Thalassiosira lentiginosa*. High concentrations of *F. kerguelensis* and *T. lentiginosa* in sediments are resistant to dissolution and associated with the ACC. However, it is difficult to extrapolate any further ecological information from the diatom evidence during this interval as it is likely to be intensely altered. Although *Pudsey and Howe* [1998] advocate stronger ACC flow during the LGM in the central Scotia Sea, the main axis of the ACC would have been displaced and ACC flow in the Falkland Trough mouth may have been much weaker than during the Holocene. In order to confirm this speculation a more extensive study of surface sediments and core records from the Falkland Trough would be necessary. However, in the absence of alternatives we propose that at the beginning of the Holocene the main axis of ACC flow became concentrated through the Falkland Trough (Figure 11c). The increased current velocities changed the settling regime at the site and resulted in the reduced sedimentation rate and the condensed Holocene sedimentary sequence.

7. Conclusions

[60] Diatomaceous sediments from core KC073 in the Falkland Trough contain evidence that variations in paleoceanographic conditions have occurred over a range of timescales since the LGM. The main conclusions of the study can be summarized as follows:

[61] 1. On the basis of the abundance proxy defined by *Gersonde and Zielinski* [2000] the record of sea ice diatoms in KC073 indicates that average winter sea ice edge was a minimum of 5° latitude farther north at the LGM than at present.

[62] 2. Seasonal sea ice cover over the site continued until approximately 19.2 ka.

[63] 3. During the early deglacial, a productivity decline between ~19.2 and 16.5 ka documents a period of open ocean conditions over the site. The Polar Front remained north of the site and an open ocean environment prevailed during this time.

[64] 4. Submillennial variations in the abundance of *Chaetoceros* rs, *Fragilariopsis kerguelensis* and *Thalassiosira antarctica* during the late glacial are inferred to relate to shifts in the path of the ACC and in the strength of NADW overflow in the Falkland Trough region, and document an important interhemispheric link between the North Atlantic and the Southern Ocean.

[65] 5. High productivity prevailed during the late deglacial until at least 12 ka when the sedimentary record becomes condensed.

[66] 6. During the Holocene, ACC velocities over the site have been sufficient to inhibit sedimentation and may have actively winnowed sediments away from the site.

References

Abelmann, A., and R. Gersonde (1988), *Cycladophora davisiana* stratigraphy in Plio-Pleistocene cores from the Antarctic Ocean (Atlantic sector), *Micropaleontology*, *34*, 268–276.

Allen, C. S. (2003), Late Quaternary Palaeoceanography of the Scotia Sea, southwest Atlantic: Evidence from the diatom record, Ph.D. thesis, Cardiff Univ., Cardiff, U. K.

Anderson, J. B. (1999), *Antarctic Marine Geology*, Cambridge Univ. Press, New York.

Andres, M. S., S. M. Bernasconi, J. A. McKenzie, and U. Rohl (2003), Southern Ocean deglacial record supports global Younger Dryas, *Earth Planet. Sci. Lett.*, *216*, 515–524.

Andrews, J. T., E. W. Domack, W. L. Cunningham, A. Leventer, K. J. Licht, A. J. T. Jull, D. J. DeMaster, and A. E. Jennings (1999), Problems and possible solutions concerning radiocarbon dating of surface marine sediments, Ross Sea, Antarctica, *Quat. Res.*, *52*, 206–216.

Arhan, M., A. C. N. Garabato, K. J. Heywood, and D. P. Stevens (2002), The Antarctic Circumpolar Current between the Falkland Islands and South Georgia, *J. Phys. Oceanogr.*, *32*, 1914–1931.

Armand, L. (1997), The use of diatom transfer functions in estimating sea-surface temperature and sea-ice in cores from the southeast Indian Ocean, Ph.D. thesis, Aust. Natl. Univ., Canberra, ACT.

Armand, L. K., and U. Zielinski (2001), Diatom species of the genus *Rhizosolenia* from Southern Ocean sediments: Distribution and taxonomic notes, *Diatom Res.*, *16*, 259–294.

Australian Antarctic Data Centre (2000), Antarctica and the Southern Ocean, *Map 12183*, Dep. of the Environ. and Heritage, Canberra, ACT.

Berkman, P. A., and S. L. Forman (1996), Pre-bomb radiocarbon and the reservoir correction for calcareous marine species in the Southern Ocean, *Geophys. Res. Lett.*, *23*, 363–366.

Bond, G. C. (1995), Oceanography—Climate and the conveyor, *Nature*, *377*, 383–384.

Brathauer, U., A. Abelmann, R. Gersonde, H. S. Niebler, and D. K. Futterer (2001), Calibration of *Cycladophora davisiana* events versus oxygen isotope stratigraphy in the subantarctic Atlantic Ocean—A stratigraphic tool for carbonate-poor Quaternary sediments, *Mar. Geol.*, *175*, 167–181.

Broecker, W. S. (1997), Thermohaline circulation, the Achilles heel of our climate system: Will man-made CO_2 upset the current balance?, *Science*, *278*, 1582–1588.

Burckle, L. H. (1984), Ecology and paleoecology of the marine diatom *Eucampia antarctica* (Castr.) Mangin, *Mar. Micropaleontol.*, *9*, 77–86.

Burckle, L. H., and R. W. Burak (1988), Fluctuations in Late Quaternary diatom abundances—Stratigraphic and paleoclimatic implication from sub-antarctic deep-sea cores, *Palaeogeogr. Palaeoclimatol. Palaeoecol.*, *67*, 147–156.

Burckle, L. H., and J. Cirilli (1987), Origin of diatom ooze belt in the Southern Ocean—Implications for Late Quaternary paleoceanography, *Micropaleontology*, *33*, 82–86.

Burckle, L. H., and D. W. Cooke (1983), Late Pleistocene *Eucampia antarctica* abundance stratigraphy in the Atlantic sector of the Southern Ocean, *Micropaleontology*, *29*, 6–10.

Crosta, X., J.-J. Pichon, and M. Labracherie (1997), Distribution of *Chaetoceros* resting spores in modern peri-Antarctic sediments, *Mar. Micropaleontol.*, *29*, 283–299.

Crosta, X., J.-J. Pichon, and L. H. Burckle (1998a), Application of modern analog technique to marine Antarctic diatoms: Reconstruction of maximum sea-ice extent at the Last Glacial Maximum, *Paleoceanography*, *13*, 284–297.

Crosta, X., J.-J. Pichon, and L. H. Burckle (1998b), Reappraisal of Antarctic seasonal sea-ice at the Last Glacial Maximum, *Geophys. Res. Lett.*, *25*, 2703–2706.

Crosta, X., A. Sturm, L. Armand, and J.-J. Pichon (2004), Late Quaternary sea ice history in the Indian sector of the Southern Ocean as recorded by diatom assemblages, *Mar. Micropaleontol.*, *50*, 209–223.

Cunningham, W. L., and A. Leventer (1998), Diatom assemblages in surface sediments of the Ross Sea: Relationship to present oceanographic conditions, *Antarct. Sci.*, *10*, 134–146.

DeFelice, D. R., and S. W. Wise (1981), Surface lithofacies, biofacies and diatom diversity patterns as models for delineation of climatic change in the south east Atlantic Ocean, *Mar. Micropaleontol.*, *6*, 29–70.

Delmonte, B., J. R. Petit, and V. Maggi (2002), Glacial to Holocene implications of the new 27000-year dust record from the EPICA Dome C (East Antarctica) ice core, *Clim. Dyn.*, *18*, 647–660.

Domack, E. W., T. A. Mashiotta, and L. A. Burkley (1993), 300-years cyclicity in organic matter preservation in Antarctic fjord sediments, in *The Antarctic Paleoenvironment: A Perspective on Global Change Part 2*, *Antarct. Res. Ser.*, vol. 60, edited by J. P. Kennett and D. A. Warnke, pp. 265–272, AGU, Washington, D. C.

Domack, E., P. O'Brien, P. Harris, F. Taylor, P. G. Quilty, L. De Santis, and B. Raker (1998), Late Quaternary sediment facies in Prydz Bay, East Antarctica and their relationship to glacial advance onto the continental shelf, *Antarct. Sci.*, *10*, 236–246.

Domack, E., A. Leventer, R. Dunbar, F. Taylor, S. Brachfeld, and C. Sjunneskog (2001), Chronology of the Palmer Deep site, Antarctic Peninsula: A Holocene palaeoenvironmental reference for the circum-Antarctic, *Holocene*, *11*, 1–9.

Dunbar, R. B., J. B. Anderson, E. W. Domack, and S. S. Jacobs (1985), Oceanographic influences on sedimentation along the Antarctic continental shelf, in *Oceanology of the Antarctic Shelf*, *Antarct. Res. Ser.*, vol. 43, edited by S. S. Jacobs, pp. 291–312, AGU, Washington, D. C.

Fryxell, G. A., G. J. Doucette, and G. F. Hubbard (1981), The genus *Thalassiosira*—The bipolar diatom *Thalassiosira-antarctica* comber, *Bot. Mar.*, *24*, 321–335.

Garabato, A. C. N., K. J. Heywood, and D. P. Stevens (2002), Modification and pathways of Southern Ocean Deep Waters in the Scotia Sea, *Deep Sea Res., Part I*, *49*, 681–705.

Gersonde, R., and U. Zielinski (2000), The reconstruction of late Quaternary Antarctic sea-ice distribution—The use of diatoms as a proxy for sea-ice, *Palaeogeogr. Palaeoclimatol. Palaeoecol.*, *162*, 263–286.

Gersonde, R., et al. (2003), Last glacial sea surface temperatures and sea-ice extent in the Southern Ocean (Atlantic-Indian sector): A multiproxy approach, *Paleoceanography*, 18(3), 1061, doi:10.1029/2002PA000809.

Harris, P. T. (2000), Ripple cross-laminated sediments on the East Antarctic Shelf: Evidence for episodic bottom water production during the Holocene?, *Mar. Geol.*, 170, 317–330.

Hays, J. D., J. A. Lozano, N. J. Shackleton, and G. Irving (1976), Reconstruction of the Atlantic and western Indian Ocean sectors of the 18,000 BP Antarctic Ocean, in *Investigation of Late Quaternary Paleoceanography and Paleoclimatology*, edited by R. M. Cline and J. D. Hays, pp. 337–372, Geol. Soc. of Am., Boulder, Colo.

Hellmer, H. H., and A. Beckmann (2001), The Southern Ocean: A ventilation contributor with multiple sources, *Geophys. Res. Lett.*, 28, 2927–2930.

Jordan, R. W., and C. J. Pudsey (1992), High-resolution diatom stratigraphy of Quaternary sediments from the Scotia Sea, *Mar. Micropaleontol.*, 19, 201–217.

Jouzel, J., et al. (1995), The 2-step shape and timing of the last deglaciation in Antarctica, *Clim. Dyn.*, 11, 151–161.

Jouzel, J., et al. (2001), A new 27 ky high resolution East Antarctic climate record, *Geophys. Res. Lett.*, 28, 3199–3202.

Kovach, W. L. (1999), *MVSP—A Multivariate Statistical Package for Windows*, version 3.1, Kovach Comput. Serv., Pentraeth, U. K.

Leventer, A. (1998), The fate of Antarctic "sea ice diatoms" and their use as paleoenvironmental indicators, in *Antarctic Sea Ice: Biological Processes, Interactions and Variability*, *Antarct. Res. Ser.*, vol. 73, edited by M. Lizotte and K. R. Arrigo, pp. 121–137, AGU, Washington, D. C.

Leventer, A., and R. B. Dunbar (1996), Factors influencing the distribution of diatoms and other algae in the Ross Sea, *J. Geophys. Res.*, 101, 18,489–18,500.

Leventer, A., E. W. Domack, S. E. Ishman, S. Brachfeld, C. E. McClennen, and P. Manley (1996), Productivity cycles of 200–300 years in the Antarctic Peninsula region: Understanding linkages among the Sun, atmosphere, oceans, sea ice, and biota, *Geol. Soc. Am. Bull.*, 108, 1626–1644.

Leventer, A., E. Domack, A. Barkoukis, B. McAndrews, and J. Murray (2002), Laminations from the Palmer Deep: A diatom-based interpretation, *Paleoceanography*, 17(3), 8002, doi:10.1029/2001PA000624.

Macdonald, A. M. (1998), The global ocean circulation: A hydrographic estimate and regional analysis, *Progr. Oceanogr.*, 41, 281–382.

Malej, A., P. Mozetic, V. Malacic, S. Terzic, and M. Ahel (1995), Phytoplankton responses to fresh-water inputs in a small semienclosed gulf (Gulf of Trieste, Adriatic Sea), *Marine Ecol. Prog. Ser.*, 120, 111–121.

Moreton, S. G. (1999), Tephrochronology of the Scotia Sea and Bellinghausen Sea, Antarctica, Ph.D. thesis, Cheltenham and Gloucester Coll. of Higher Educ., Cheltenham, U. K.

Ninnemann, U. S., C. D. Charles, and D. A. Hodell (1999), Origin of global millennial scale climate events: Constraints from the Southern Ocean deep sea sedimentary record, in *Mechanisms of Global Climate Change at Millennial Time Scales*, *Geophys. Monogr. Ser.*, vol. 112, edited by P. U. Clark, R. S. Webb, and L. D. Keigwin, pp. 99–112, AGU, Washington D. C.

Olbers, D., V. V. Gouretski, G. Seiss, and J. Schroter (1992), *Hydrographic Atlas of the Southern Ocean*, p. xvii, Alfred Wegner Inst., Bremerhaven, Germany.

Orsi, A. H., T. Whitworth III, and W. D. Nowlin Jr (1995), On the meridional extent and fronts of the Antarctic Circumpolar Current, *Deep Sea Res., Part I*, 42, 641–673.

Pahnke, K., R. Zahn, H. Elderfield, and M. Schulz (2003), 340,000-year centennial-scale marine record of Southern Hemisphere climatic oscillation, *Science*, 301, 948–952.

Peterson, R. G., and T. Whitworth (1989), The Subantarctic and Polar Fronts in relation to deep water masses through the southwestern Atlantic, *J. Geophys. Res.*, 94, 10,817–10,838.

Pichon, J. J., M. Labracherie, L. D. Labeyrie, and J. Duprat (1987), Transfer-function between diatom assemblages and surface hydrology in the Southern Ocean, *Palaeogeogr. Palaeoclimatol. Palaeoecol.*, 61, 79–95.

Piotrowski, A. M., S. L. Goldstein, S. R. Hemming, and R. G. Fairbanks (2004), Intensification and variability of ocean thermohaline circulation through the last deglaciation, *Earth Planet. Sci. Lett.*, 225, 205–220.

Pudsey, C. J. (1993), Calibration of a point-counting technique for estimation of biogenic silica in marine sediments, *J. Sediment. Petrol.*, 63, 760–762.

Pudsey, C. J., and J. Evans (2001), First survey of Antarctic sub-ice shelf sediments reveals mid- Holocene ice shelf retreat, *Geology*, 29, 787–790.

Pudsey, C. J., and J. A. Howe (1998), Quaternary history of the Antarctic Circumpolar Current: Evidence from the Scotia Sea, *Mar. Geol.*, 148, 83–112.

Rosqvist, G. C., and P. Schuber (2003), Millennial-scale climate changes on South Georgia, Southern Ocean, *Quat. Res.*, 59, 470–475.

Round, F. E., R. M. Crawford, and D. G. Mann (1990), *The Diatoms, Biology and Morphology of the Genera*, Cambridge Univ. Press, New York.

Scherer, R. P. (1994), A new method for the determination of absolute abundance of diatoms and other silt-sized sedimentary particles, *J. Paleolimnol.*, 12, 171–179.

Schmittner, A., O. A. Saenko, and A. J. Weaver (2003), Coupling of the hemispheres in observations and simulations of glacial climate change, *Quat. Sci. Rev.*, 22, 659–671.

Seidov, D., E. Barron, and B. J. Haupt (2001), Meltwater and the global ocean conveyor: Northern versus southern connections, *Global Planet. Change*, 30, 257–270.

Shemesh, A., L. H. Burckle, and P. N. Froelich (1989), Dissolution and preservation of Antarctic diatoms and the effect on sediment thanatocoenoses, *Quat. Res.*, 31, 288–308.

Shemesh, A., D. Hodell, X. Crosta, S. Kanfoush, C. Charles, and T. Guilderson (2002), Sequence of events during the last deglaciation in Southern Ocean sediments and Antarctic ice cores, *Paleoceanography*, 17(4), 1056, doi:10.1029/2000PA000599.

Sjunneskog, C., and F. Taylor (2002), Postglacial marine diatom record of the Palmer Deep, Antarctic Peninsula (ODP Leg 178, Site 1098): 1. Total diatom abundance, *Paleoceanography*, 17(3), 8003, doi:10.1029/2000PA000563.

Skinner, L. C., and I. N. McCave (2003), Analysis and modelling of gravity and piston coring based on soil mechanics, *Mar. Geol.*, 199, 181–204.

Smetacek, V., C. Klaas, S. Menden-Deuer, and T. Rynearson (2002), Mesoscale distribution of dominant diatom species relative to the hydrological field along the Antarctic Polar Front, *Deep Sea Res., Part II*, 49, 3835–3848.

Stuiver, M., and P. D. Quay (1981), A 1600-year-long record of solar change derived from atmospheric C-14 levels, *Sol. Phys.*, 74, 479–481.

Stuiver, M., and P. J. Reimer (1993), Extended ^{14}C data base and revised calib 3.0 ^{14}C age calibration program, *Radiocarbon*, 35, 215–230.

Stuiver, M., P. J. Reimer, E. Bard, J. W. Beck, G. S. Burr, K. A. Hughen, B. Kromer, G. McCormac, J. Van der Plicht, and M. Spurk (1998), INTCAL98 radiocarbon age calibration, 24,000–0 cal BP, *Radiocarbon*, 40, 1041–1083.

Taylor, F., and A. McMinn (2002), Late Quaternary diatom assemblages from Prydz Bay, eastern Antarctica, *Quat. Res.*, 57, 151–161.

Taylor, F., and C. Sjunneskog (2002), Postglacial marine diatom record of the Palmer Deep, Antarctic Peninsula (ODP Leg 178, Site 1098): 2. Diatom assemblages, *Paleoceanography*, 17(3), 8001, doi:10.1029/2000PA000564.

Taylor, F., J. Whitehead, and E. Domack (2001), Holocene paleoclimatic change in the Antarctic Peninsula: Evidence from the diatom, sedimentary and geochemical record, *Mar. Micropaleontol.*, 41, 25–43.

Ter Braak, C. J. F., and P. Smilauer (2002), *CANOCO Reference Manual and CANODRAW for Windows User's Guide*, Biometris, Ithaca, New York.

Tremblay, J. E., M. I. Lucas, G. Kattner, R. Pollard, V. H. Strass, U. Bathmann, and A. Bracher (2002), Significance of the Polar Frontal Zone for large-sized diatoms and new production during summer in the Atlantic sector of the Southern Ocean, *Deep Sea Res. Part II*, 49, 3793–3811.

Villareal, T. A., and G. A. Fryxell (1983), Temperature effects on the valve structure of the bipolar diatoms *Thalassiosira antarctica* and *Porosira glacialis*, *Polar Biol.*, 2, 163–169.

Waelbroeck, C., J. Duplessy, E. Michel, L. Labeyrie, D. Paillard, and J. Duprat (2001), The timing of the last deglaciation in North Atlantic climate records, *Nature*, 412, 724–727.

Wang, Z., L. A. Myask, and J. F. McManus (2002), Response of the thermohaline circulation to cold climates, *Paleoceanography*, 17(1), 1006, doi:10.1029/2000PA000587.

Warner, N. R., and E. Domack (2002), Millennial- to decadal-scale paleoenvironmental change during the Holocene in the Palmer Deep, Antarctica, as recorded by particle size analysis, *Paleoceanography*, 17(3), 8004, doi:10.1029/2000PA000602.

Zielinski, U., and R. Gersonde (1997), Diatom distribution in Southern Ocean surface sediments (Atlantic sector): Implications for paleoenvironmental reconstructions, *Palaeogeogr. Palaeoclimatol. Palaeoecol.*, 129, 213–250.

Zielinski, U., R. Gersonde, R. Sieger, and D. Futterer (1998), Quaternary surface water temperature estimations: Calibration of a diatom transfer function for the Southern Ocean, *Paleoceanography*, 13, 365–383.

————————

C. S. Allen and C. J. Pudsey, British Antarctic Survey, High Cross, Madingley Road, Cambridge CB3 0ET, UK. (c.allen@bas.ac.uk)

A. Leventer, Department of Geology, Colgate University, 13 Oak Drive, Hamilton, NY 13346, USA.

J. Pike, Department of Earth Sciences, Cardiff University, Earth Sciences, Park Place, P.O. Box 914, Cardiff CF10 3YE, UK.